GUIDELINE OF PERFORMANCE TEST AND EVALUATION ON ULTRASOUND DIAGNOSTIC EQUIPMENT USING LINEAR AND SECTOR TRANSDUCERS ON ATS539 MULTIPURPOSE PHANTOM

N. Ibrahim[1,*], D. Asyraf Anuar[1] and J. Natasya Akmal[1] and M. Rabani Adnan[2]

[1]Department of Electronic Engineering,
Faculty of Electrical and Electronic Engineering
Universiti Tun Hussein Onn Malaysia
[2]Department of Laboratory Management and Asset
Faculty of Electrical and Electronic Engineering
Universiti Tun Hussein Onn Malaysia

[*]Corresponding Author's Email: [1]nabilah@uthm.edu.my

Article History: Received February 11, 2026; Revised May 5, 2026; Accepted May 31, 2026

ABSTRACT: Routine performance testing is critical for ensuring ultrasound diagnostic accuracy, yet standardized guidelines for multi-transducer evaluation remain limited. This study addresses this gap by proposing a systematic performance evaluation guideline for the Canon Aplio Me system using PLU-805BT linear and PSU-30BT sector transducers on an ATS539 multipurpose phantom. The framework assesses key parameters, including axial and lateral resolution, geometric calibration, and grayscale dynamic range. Results indicate that the linear transducer (10–12 MHz) achieves superior resolution, with errors below 1%, while the sector transducer (3–5 MHz) enables deeper penetration, with errors up to 6%. These findings indicate high system accuracy across a range of operating frequencies. This research contributes a reproducible methodology for ultrasound quality assurance, providing a standardized approach to support clinical maintenance, educational training, and diagnostic reliability in research settings

KEYWORDS: *Multipurpose Phantom; Ultrasound Diagnostic Equipment; Axial Lateral Resolution; Grayscale Dynamic Range; Objective Quality Assurance.*

1.0 INTRODUCTION

The diagnostic accuracy and reliability of ultrasound imaging are in high demand due to its real-time capability, portability, and non-invasive nature. Although it has become a gold standard for clinical examinations, its effectiveness remains heavily dependent on the technical performance of the ultrasound system and the specific transducers used [1]-[3]. Despite its widespread use, formal quality assurance remains inconsistent across clinical settings, with many facilities lacking standardized protocols [4][5]. A critical issue is that modern signal processing often masks subtle hardware faults or gradual performance degradation, leading users to believe the equipment is functioning correctly when it is not [5]. Empirical evidence indicates that ultrasound transducers in clinical practice experience an annual failure rate of 10–13%, with some studies identifying defects in up to 40% of tested probes [1]. These defects can lead to significant measurement inaccuracies and potential misdiagnosis [1].

Furthermore, while multipurpose phantoms are utilized for system calibration, there are currently no universally accepted standard protocols for evaluating linear and sector transducers across a broad frequency range [6]. Specific parameters, such as horizontal distance accuracy, are particularly prone to falling outside of tolerance ranges during objective evaluations [7]. This situation highlights an urgent need to develop reproducible, objective guidelines to ensure long-term diagnostic reliability. To address these gaps, this study provides a systematic evaluation guideline for the Canon Aplio Me system using linear and sector transducers on the ATS539 multipurpose phantom. By assessing parameters such as axial/lateral resolution and geometric calibration, this research establishes a framework for objective quality control. The results of this evaluation indicate high system accuracy across a range of frequencies, offering a reproducible methodology that supports clinical maintenance, standardized training, and early detection of equipment failure.

2.0 METHODOLOGY – MULTIPURPOSE PHANTOM AND ULTRASOUND DIAGNOSTIC EQUIPMENT AS DATA SOURCES

2.1 Equipment and Phantom Description

The performance evaluation was conducted using the Canon Aplio Me diagnostic ultrasound system (Figure 1). It integrates beamforming, signal processing, and image optimization technologies to deliver high-resolution B-mode imaging. Two transducers were evaluated to cover a broad range of clinical applications: a PLU-805BT linear transducer (10–12 MHz) for high-resolution superficial imaging and a PSU-30BT sector transducer (3–5 MHz) for deeper penetration. The evaluation utilized the ATS539 Multipurpose Phantom (Figure 2), which contains tissue-mimicking material with a propagation speed of 1450 m/s [6]. The phantom features specialized target groups, including monofilament line targets for axial and lateral resolution, geometric calibration targets, and grayscale structures for dynamic range assessment [7], as shown in the schematic design in Figure 3. The design thus allows comprehensive assessment of key imaging parameters, such as axial and lateral resolution, contrast resolution, measurement accuracy, and transducer sensitivity, under controlled conditions. Here, the evaluation was prioritized to axial/lateral resolution, vertical and horizontal measurements, and grayscale and dynamic range that are relevant to clinical applications and the physical characteristics of ultrasound imaging.

Figure 1: Canon Aplio Me ultrasound diagnostic equipment system associated with linear and sector transducers.

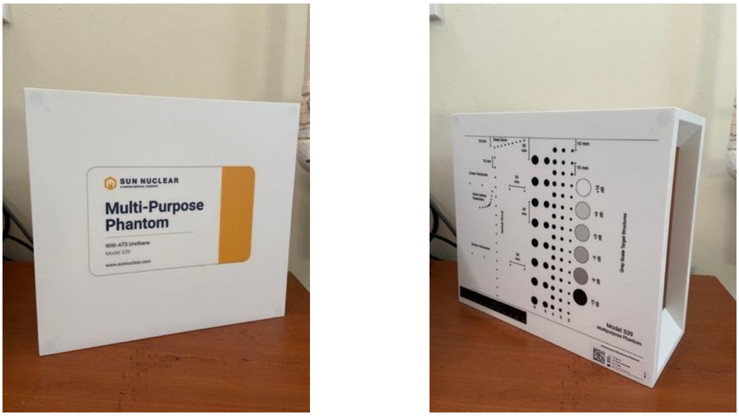

(a) front view (b) back view

Figure 2: Multipurpose phantom ATS539 from (a) front view and (b) back view.

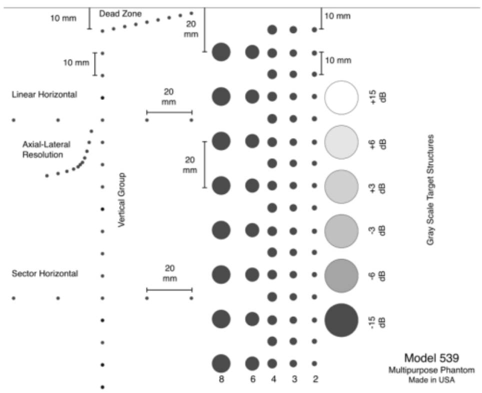

Figure 3: Target schematic of multipurpose phantom ATS539

2.2 Experimental Setup and Parameter Justification

To ensure consistency and reproducibility across all tests, the system was configured with a dedicated Quality Assurance preset [8]. The following parameters were standardized:

Mechanical Index at 0.9: This setting provides sufficient acoustic power to achieve a high signal-to-noise ratio for deep-target visualization while remaining well within clinical safety limits [8]. Standardizing the MI is critical for longitudinal performance tracking, as it ensures consistent beam intensity across different evaluation sessions [7].

Gain at 80: A fixed gain of 80 was chosen to provide high sensitivity for detecting low-contrast targets and the distal edges of phantom structures without causing signal saturation [9]. By turning off automatic gain compensation and setting a fixed baseline, subtle hardware degradations are more easily detected [4].

Dynamic Range at 60: This setting was selected to provide balanced grayscale contrast, allowing clear differentiation of the 6-step grayscale targets within the phantom. A DR of 60 ensures that transitions between varying echo intensities are visible, supporting an objective assessment of the system's signal-processing accuracy [10].

2.3 Measurement Procedure and Error Calculation

All measurements were obtained manually using the ultrasound system's built-in electronic calipers. For each parameter, the transducer was positioned over the relevant target array on the phantom. Once a clear image was captured, the display was frozen, and the calipers were placed at the leading edges of the targets to measure the distance. To evaluate the accuracy of these measurements against the phantom's known ground truth, the Mean Squared Error was calculated. MSE is a preferred metric as it penalizes larger outlier errors, providing a clear indication of system reliability. The formula used for MSE is:

$$MSE = \frac{1}{n}\sum_{i=1}^{n}\left(d_{measured,i} - d_{actual,i}\right)^2$$

Where:

n is the total number of measurements taken for a specific parameter,

$d_{measured,i}$ is the distance recorded by the ultrasound system calipers and $d_{actual,i}$ is the true distance specified in the ATS539 phantom documentation.

3.0 MEASUREMENT RESULTS AND DISCUSSION

3.1 Axial and Lateral Resolutions

Axial resolution refers to the minimum distance between two closely spaced reflectors along the direction of the ultrasound beam that allows them to be distinguished as separate structures. In contrast, lateral resolution describes the system's ability to resolve objects positioned side by side, perpendicular to the direction of the sound beam. In case the ultrasound system has poor resolution, small structures that are close together may appear as a single image, potentially leading to misinterpretation of the findings. Figure 4 shows the schematic line targets in the phantom for the axial and lateral arrays, with the actual distances also tabulated in Table 1.

The transducer center frequency, damping properties, and pulse length influence axial resolution. In general, higher frequencies produce better axial resolution. Meanwhile, lateral resolution is largely determined by the beam width. It varies with imaging depth, transducer focusing characteristics, the number of scan lines used, and the system sensitivity and gain settings. Thus, by considering multiple frequencies for the linear and sector transducers, varying imaging depths are set up to measure the axial and lateral arrays. Figure 5 shows the results of B-mode axial and lateral resolution images, both obtained by the linear and sector transducers. Linear transducer capable of producing clear resolution when operating at 10 MHz and 12 MHz.

Meanwhile, the sector transducer operates at 3 MHz and 5 MHz to view the axial and lateral arrays. Both sample images have significantly different depths due to the frequency's penetration. The performance of the Canon Aplio Me system was evaluated using both the linear and sector transducers. The linear transducer successfully resolved the axial and lateral targets with errors of less than 1% compared to the phantom's known distances. In contrast, the sector transducer exhibited higher error rates, remaining below 4% for most measurements. Notably, at the 3 MHz frequency setting, the lateral targets became too blurry to be measured accurately. The sample images in Figure 5 illustrate the significant difference in imaging depth between the two transducers, due to frequency-dependent penetration.

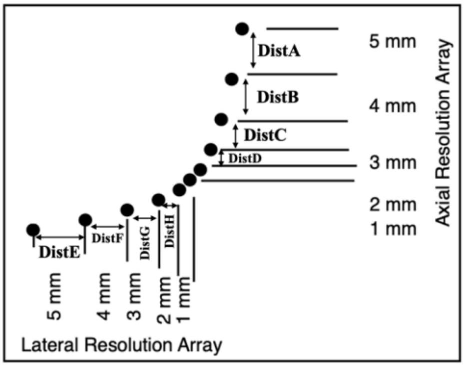

Figure 4: Target schematic on axial-lateral resolution array

Table 1: The actual distance of the target in the axial and lateral resolution array

Resolution	Actual target distance
Axial	DistA = 5 mm
	DistB = 4 mm
	DistC = 3 mm
	DistD = 2 mm
Lateral	DistE = 5 mm
	DistF = 4 mm
	DistG = 3 mm
	DistH = 2 mm

Figure 5: B-mode resolution images during the measurement of distance in axial and lateral arrays using (left) a linear transducer and (right) a sector transducer. The linear transducer can scan and distinguish between the axial and lateral arrays at 10 MHz and 12 MHz. Meanwhile, the sector transducer used 3 MHz and 5 MHz to provide a clearer view of the arrays at greater depth.

3.2 Geometric Calibration: Vertical and Horizontal

Vertical distance measurements are performed along the direction of the ultrasound beam. Precise depiction of a structure's size, depth, and volume is essential for accurate diagnosis. Thus, as with lateral resolution, the calibration of vertical distance is performed by measuring the distance between two separate targets and comparing it with the known values within the phantom. Due to the linear transducer's low penetration at higher frequencies, targets deeper than 7.5 cm were not visualized, as shown in Figure 6. However, the low-frequency sector transducers at 3.5 MHz and 5.0 MHz can view deeper targets to 18 cm. As shown in Figure 1, the known distance between targets in the vertical arrays is 10 mm. Here, Tables 2 and 3 present the manually measured distances using the electronic calipers when scanned by the linear and sector transducers. The calculated mean squared error (MSE) indicated an error of less than 1% between the measured and known values. This value confirms the good accuracy of the measurements obtained with both transducers.

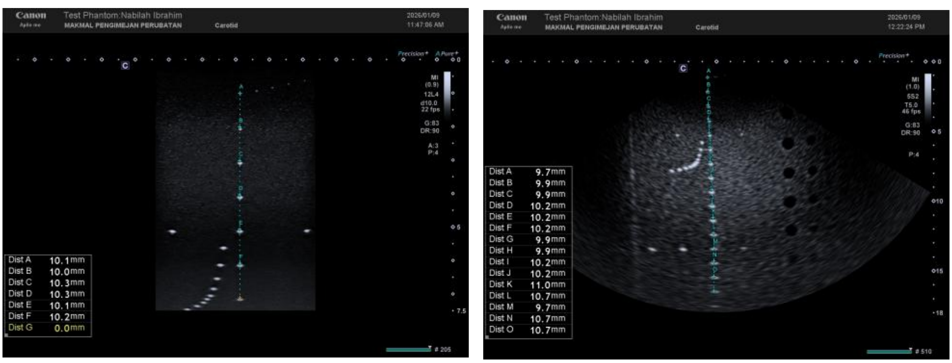

Figure 6: B-mode images during the vertical measurement of target distance using (left) a linear transducer (10 MHz) and (right) a sector transducer (5 MHz).

Table 2: The vertical distance measurement at 10 MHz using a linear transducer

Item	Frequency 10 MHz	
Vertical distance viewed until 7.5 cm depth	DistA =10.1 mm DistB =10.0 mm DistC =10.3 mm DistD =10.3 mm DistE =10.1 mm DistF =10.2 mm	<1% error

Table 3: The vertical distance measurement for multiple frequencies using a sector transducer

Item	Frequencies 3.5 MHz		Frequencies 5.0 MHz	
Vertical distance viewed until 18.0 cm depth	DistA =9.9 mm	DistI =10.2 mm	DistA =9.7 mm	DistI =10.2 mm
	DistB =9.9 mm	DistJ =9.9 mm	DistB =9.9 mm	DistJ =10.2 mm
	DistC =9.9 mm	DistK =10.2 mm	DistC =9.9 mm	DistK =11.0 mm
	DistD =10.2 mm	DistL =10.2 mm	DistD =10.2 mm	DistL =10.7 mm
	DistE =10.7 mm	DistM =10.2 mm	DistE =10.2 mm	DistM =9.7 mm
	DistF =10.4 mm	DistN =11.0 mm	DistF =10.2 mm	DistN =10.7 mm
	DistG =10.2 mm	DistO =10.7 mm	DistG =9.9 mm	DistO =10.7 mm
	DistH = 10.2 mm		DistH = 9.9 mm	
	< 1% error		<1% error	

Horizontal distance measurements are obtained perpendicular to the axis of the sound beam. Figure 7 shows the horizontal target schematic with a 20 mm spacing between targets at 5 cm depth. This area is clearly covered by a linear transducer at 10.5 MHz. As for the sector transducer with a lower frequency, a 13 mm-deep target is evaluated at 5 MHz (Figure 8). All manually measured distances are presented in Table 4 and then compared with the known distance of 20 mm for performance evaluation. Squared errors were calculated, and a value of less than 1% was obtained for the operating frequency of 10.5 MHz using a linear transducer. However, the errors for the target distance measurement in the sector horizontal region showed higher values between 4% and 12% due to the widening of the target shape in the deeper part. This observation creates ambiguity when manually determining the target's edge. This outcome is due to beam divergence and frequency-dependent attenuation.

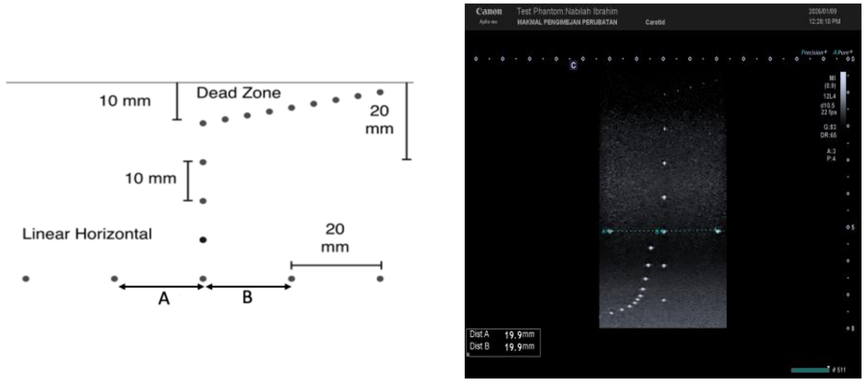

Figure 7: (Left) Target schematic on horizontal distance and (right) B-mode target phantom image scanned by 10.5 MHz linear transducer at 5 cm depth

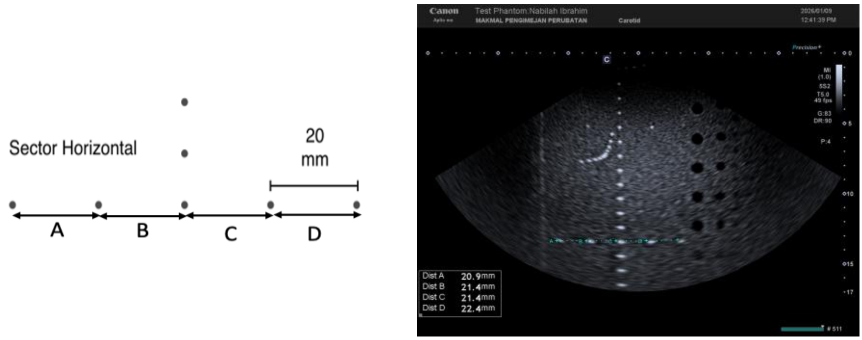

Figure 8: (Left) Target schematic on horizontal distance and (right)B-mode target phantom image scanned by a 5 MHz sector transducer at 13 cm depth.

Table 4: The horizontal distance measurement using a 10.5 MHz linear transducer and a 5 MHz sector transducer at 5 cm and 13 cm depth, respectively.

Item	Frequency 10.5 MHz	Item	Frequency 5 MHz
Horizontal distance at depth of 5 cm	DistA =19.9 mm DistB =19.9 mm	Horizontal distance at depth of 13 cm	DistA =20.9 mm DistB =21.4 mm DistC =21.4 mm DistD =22.4 mm
	< 1% error		4% - 12% error

3.3 Transducer Performance Comparison

The evaluation revealed that the PLU-805BT linear transducer (10-12 MHz) performed significantly better in terms of precision and resolution than the PSU-30BT sector transducer (3-5 MHz). The linear transducer maintained an error margin of <1% for both axial and lateral resolution at shallow depths. In contrast, the sector transducer produced errors up to 4% at 5 MHz and failed to resolve lateral targets entirely at 3 MHz due to excessive blurring. Moreover, the linear transducer achieved high horizontal accuracy (<1% error) at a depth of 5 cm. Meanwhile, the sector transducer accuracy degraded significantly at depth, reaching at 12% error at 13 cm.

3.4 Grayscale and Dynamic Range

Grayscale processing assigns varying levels of brightness to the received echo signals based on their amplitudes. The range of echo signal amplitude, from the lowest grayscale level to the highest displayable brightness, is known as the dynamic range. In clinical practice, grayscale processing and the displayed dynamic range enable the simultaneous visualization of echoes with different amplitudes within a single image. Thus, by using two different transducers of linear and sector, the known brightness of the grayscale target structure is scanned to visualize the round shapes at different grayscale levels. The brightness range is between +15dB and -15dB as guided in Figure 1. Figures 9 and 10 show the B-mode images of the grayscale target scanned with a sector transducer at 5 MHz and a linear transducer at 8 MHz. The depth of these images was significantly influenced by the transducer type and the operating frequency; the 5 MHz frequency produced an image to a depth of 14 cm, while the 8 MHz frequency from the linear transducer produced a maximum depth of 8 cm with clear target visibility. Here, low-contrast targets were easily identified with the linear transducer at shallow depths, while deeper targets showed reduced contrast recognition. Positive results of target visibility are evaluated when the targets are clearly visible as round, as summarized in Table 5. The visibility of these targets was defined as the ability to distinguish the target boundary from the background tissue-mimicking material with a distinct contrast threshold.

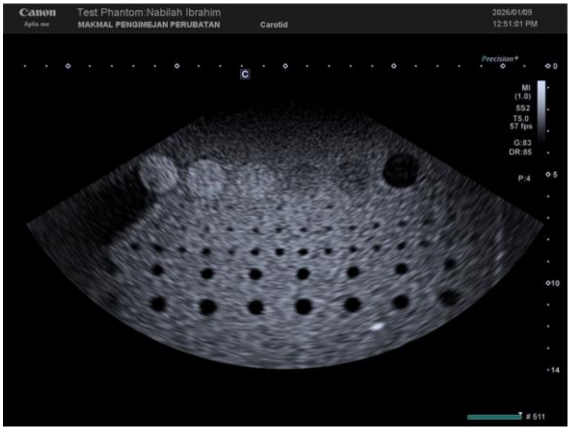

Figure 9: B-mode image grayscale target scanned by sector transducer at 5 MHz

Grayscale target of +15dB and +6dB	Grayscale target of +3dB and -3dB	Grayscale target of -6dB and -15dB
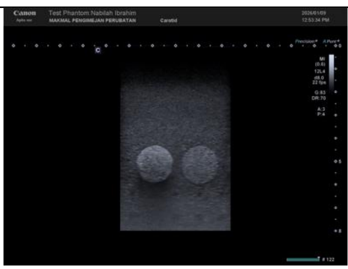	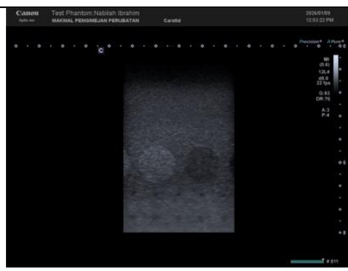	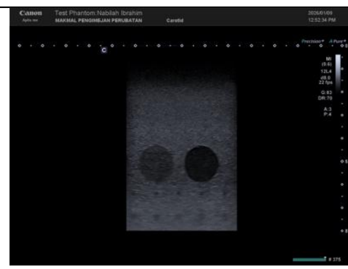

Figure 10: B-mode image grayscale target scanned by a linear transducer at 8 MHz in separate images due to the limited window length of the transducer

Table 5: Results on manually visualizing the grayscale target structure image

dB	Grayscale target scanned by sector transducer at 5 MHz (refer to Figure 9)	Grayscale target scanned by a linear transducer at 8 MHz (refer to Figure 10)
	Clearly visible as a round	
+15	✓	✓
+6	✓	✓
+3		✓
-3		✓
-6		
-15	✓	✓

4.0 DISCUSSION

The linear transducer achieving an error margin of < 1% is highly significant in the context of technical quality assurance. Most international guidelines, such as those from the BMUS and EFSUMB, set the tolerance limit for geometric calibration at 2% or 1 mm, whichever is greater [3][4]. An error below 1% indicates high system accuracy and confirms that the system's digital scan converter and internal measurement software are perfectly calibrated. This low baseline is critical because it enables early detection of subtle hardware degradation before it reaches clinically significant levels.

The performance disparity between the two transducers is primarily rooted in the physics of beam divergence. Higher-frequency transducers, such as the 12 MHz linear probe, produce a more collimated beam in the near field, minimizing "smearing" and maintaining high lateral resolution. However, as imaging depth increases, particularly with the lower-frequency (3–5 MHz) sector transducer, the ultrasound beam naturally diverges, or widens. This beam widening leads to resolution degradation, with point targets appearing as arcs rather than distinct points. This physical phenomenon explains the 12% horizontal measurement error observed at 13 cm: the targets smear, making it impossible for the user to precisely locate the leading edge with the calipers and leading to manual measurement ambiguity.

On the other side, visible targets were defined by the system's ability to maintain a sufficient Contrast-to-Noise Ratio at a Dynamic Range of 60. Quantitative visibility is determined by the system's ability to display targets ranging from -6 dB to +15 dB relative to the background

TMM. The clarity observed in Figure 9 and Figure 10 confirms that the Canon Aplio Me maintains a linear grayscale response, ensuring that subtle differences in tissue echogenicity are accurately represented and that lesions or fluid collections can be identified.

5.0 CONCLUSION

This study addresses the objective of establishing a standardized guideline for the performance testing of ultrasound diagnostic equipment using linear and sector transducers on the ATS539 multipurpose phantom. The proposed approach enables an objective, systematic evaluation of key imaging parameters and highlights performance variations across different transducer types. These findings support the development of a more consistent and reliable quality assurance framework for ultrasound systems. Future work will focus on integrating quantitative image analysis methods to enhance the robustness and comprehensiveness of ultrasound quality assurance practices.

6.0 ACKNOWLEDGMENTS

This research was supported by Universiti Tun Hussein Onn Malaysia through GPPS Research Grant (votJ040).

7.0 REFERENCES

[1] O. Oglat, "Performance evaluation of an ultrasound imaging system using tissue-mimicking phantoms for quality assurance," *Biomimetics*, vol. 7, no. 3, pp. 130–158, 2022.

[2] H. Hsu, K. A. Wear, T. J. Pfefer, and W. C. Vogt, "Tissue-mimicking phantoms for performance evaluation of photoacoustic microscopy systems," *Biomedical Optics Express*, vol. 13, pp. 1357–1373, 2022.

[3] Kollmann, C. deKorte, N.J. Dudley, "Guideline for Technical Quality Assurance (TQA) of Ultrasound Devices (B-mode)", *European Journal of Ultrasound*, vol. 33, pp. 544-549, 2012.

[4] N. Dudley, S. Russell, Ward, Hoskins, "The BMUS Guidelines for Regular Quality Assurance Teting of Ultrasound Scanners", Ultrasound, vol. 22, pp. 6-7, 2014.

[5] G. Paula, P. Vasques, S. Souza, "Quality Control in Ultrasound: Principle Recommendations Perspective," Revista, vol. 4, pp. 1-13, 2022.

[6] J. James, Jung Choi, J. Jung, "Image Quality Control for Linear Transducers with Various Frequencies by using an ATS-550 Phantom", Journal of the Korean Physical Society, vol. 70, pp. 206-212, 2017.

[7] Y. Cho, Y. Lee, L Lee, "Quality Evaluation of Ultrasonographic Equipment using an ATS-539 Multipurpose Phantom in Veterinary Medicine", vol. 39, pp. 114-120, 2022.

[8] E. Sassaroli, A. Scorza, C. Crake, S. A. Sciuto, "Breast Ultrasound Technology and Performance Evaluation of Ultrasound Equipment: B-mode," *IEEE Transaction on Ultrasonics, Ferroelectrics, and Frequency Control*, pp. 1–14, 2016.

[9] K. Kanal, J. Kofler, D. Groth, "Comparison of Selected Ultrasound Performance Tests with Vrying Overall Receiver Gain and Dynamic Range using Conventional and Magnified Field of View," *International Journal of Medical Physics Research and Practice*, vol. 25, pp. 642-647, 1998.

[10] G. Moore, A. Gessert, M. Schafer, "The Need for Evidence-Based Quality Assurance in the Modern Ultrasound Clinical Laboratory," *Ultrasound*, vol. 13, pp. 158-162, 2005.